PHILOSOPHICAL TRANSACTIONS OF THE ROYAL SOCIETY A MATHEMATICAL, PHYSICAL & ENGINEERING SCIENCES

Satellite Ozone Measurements

A. J. Krueger, B. Guenther, A. J. Fleig, D. F. Heath, E. Hilsenrath, R. McPeters and C. Prabhakara

Phil. Trans. R. Soc. Lond. A 1980 **296**, 191-204
doi: 10.1098/rsta.1980.0164

Phil. Trans. R. Soc. Lond. A **296**, 191–204 (1980) [191]
Printed in Great Britain

Satellite ozone measurements

By A. J. Krueger, B. Guenther, A. J. Fleig, D. F. Heath, E. Hilsenrath, R. McPeters and C. Prabhakara
Laboratory for Atmospheric Sciences, Goddard Space Flight Center, Greenbelt, Maryland 20771 *U.S.A.*

Three classes of ozone sounders have been developed since the first Echo Satellite measurements in 1960. They are the (1) backscatter ultraviolet (b.u.v.), (2) infrared limb and nadir radiance, and (3) stellar and solar occultation methods. With these techniques, ozone has been measured from 20 to 100 km. Tropospheric ozone measurements are beyond present technology, but total ozone is determined with the b.u.v. and nadir infrared methods.

Results from the occultation methods are excessively variable, indicating a need for refinement of the technique. Evidence from this technique for a mesospheric ozone maximum is strong. The most extensive set of ozone observations has come from the Nimbus 4 b.u.v. between 1970 and 1977. From this and earlier b.u.v. experiments, it has been determined that the ozone tends toward photochemical steady state densities for levels above 5 mbar and that the temperature coefficient near 1 mbar is approximately 1000 K, in accordance with odd hydrogen catalysis of ozone. At lower altitudes, odd nitrogen catalytic chemistry has been verified from b.u.v. ozone observations during a solar proton event. Ozone profile results from the limb infrared radiance method are discussed in a companion paper by Dr J. C. Gille.

Total ozone soundings from the b.u.v. agree with Dobson results and details of seasonal and latitudinal variations are now available. The total ozone field has also been inferred from nadir infrared radiance data. Monthly mean total ozone maps from this method and the b.u.v. each indicate standing waves at all latitudes.

Introduction

In the last 15 years, interest in stratospheric ozone has changed from scientific curiosity to the present need for monitoring for environmental reasons. Fortunately, a variety of remote ozone sounding techniques were proposed and tested with satellites during the 1960s and early 1970s so that the current needs for research and climatological data can be met with a combination of satellite and conventional sounding devices. This paper is a review of satellite methods and, in conjunction with Dr Gille's paper, a summary of principal findings.

Ozone molecules absorb radiation strongly in the middle ultraviolet (u.v.) Hartley–Huggins bands (220–320 nm), moderately in the infrared (9.6 μm), and weakly in the visible Chappuis bands (0.6 μm). Perhaps the first measurement of ozone to use artificial Earth satellites in connection with the selective absorption of light employed the Echo balloon satellite. Sunlight in the Chappuis band wavelengths which passed through the Earth's limb was measured with a ground based telescope after reflexion from the satellite (Venkateswaran *et al.* 1961). A useful remote sounding technique, namely *limb occultation*, was demonstrated, although, because of geometric problems, the resulting ozone profiles were incorrect. This technique, as with most others, had a pre-satellite origin; that of lunar eclipse photometry. A chronology of developments in limb occultation methods and in the other major satellite techniques for ozone measurement is given in table 1.

The second major remote sensing method to be proposed was the *backscatter ultraviolet* (b.u.v.) technique. Sunlight in the Hartley–Huggins bands penetrates to various stratospheric altitudes (which depend on the wavelength-dependent ozone absorption cross section) where the photons are either absorbed or Rayleigh scattered. Measurements of the Earth albedo at several u.v. wavelengths can yield an ozone profile. The method was proposed by Singer & Wentworth (1957) and newer methods for inversion of the albedo measurements have been developed and reviewed by Mateer (1972). An important extension of the b.u.v. method was to measure total ozone as suggested by Dave & Mateer (1967).

TABLE 1. SATELLITE EXPERIMENTS TO MEASURE OZONE

type	satellite	wavelengths nm	latitude coverage	comments	references
occultation					
solar	Echo 1	590, 529.5	17 N	Dec. 1960	Venkateswaran *et al.* (1961)
	U.S.A.F. 1962	260	33 S–13 S	July 1962	Rawcliffe *et al.* (1963)
	Ariel 2	200–400	50 S–50 N	April, May, Aug. 1964	Miller & Stewart (1965)
	AE-5	255.5	5 N	Dec. 1976	Guenther *et al.* (1977)
stellar	OAO-2	250	16 S–43 N	Jan. 1970, Aug. 1971	Hays & Roble (1973)
	OAO-3	258–343	12 S–3 N	July 1975	Riegler *et al.* (1976)
backscatter u.v.					
profile	U.S.A.F. 1965	284	60 S–60 N	Feb.–Mar. 1965	Rawcliffe & Elliott (1966)
	U.S.S.R.	225–307	60 S–60 N	Apr. 1965	Iozenas *et al.* (1969)
		250–330	60 S–60 N	June 1966	Iozenas *et al.* (1969)
	1966-111 B	175–310	80 S–80 N	1966	Elliott *et al.* (1967)
	OGO-4	110–340	80 S–80 N	Sept. 1967–Jan. 1969	Anderson *et al.* (1969)
	Nimbus 4 b.u.v.	255.5–305.8	80 S–80 N	Apr. 1970–July 1977	Heath *et al.* (1973)
	AE-5 b.u.v.	255.5–305.8	20 S–20 N	Nov. 1975–Apr. 1977	Frederick *et al.* (1977*a*)
	Nimbus 7 s.b.u.v.	255.5–305.8	80 S–80 N	Nov. 1978*	Heath *et al.* (1975)
total	Nimbus 4 b.u.v.	312.5–339.8	80 S–80 N	Apr. 1970–July 1977	Mateer *et al.* (1971)
	AE-5 b.u.v.	312.5–339.8	20 S–20 N	Nov. 1974–Apr. 1976	
	Nimbus 7 t.o.m.s.	312.5–339.8	global	Nov. 1978*	Heath *et al.* (1975)
infrared emission		μm			
profile	Nimbus 6 l.r.i.r.	9.6	65 S–90 N	June 1975–Jan. 1976	Gille (1979, this symposium)
	Nimbus 7 l.i.m.s.	9.6	65 S–90 N	Oct. 1978–May 1979	Nimbus project (1978)
total	Nimbus 3 i.r.i.s.	9–10 spectral scan	80 S–80 N		Hanel *et al.* (1970)
	Nimbus 4 i.r.i.s.	9–10 spectral scan	80 S–80 N	Apr. 1970–Jan. 1971	Prabhakara *et al.* (1976)
	Block 5 m.f.r. (4 flights)		global	Mar. 1977*	Lovill *et al.* (1978)
	Tiros *N* h.i.r.s.	9.71	global	Nov. 1978*	

* Currently in operation (Nov. 1979).

Satellite measurements of ozone profiles by the backscatter method were first made by Iozenas *et al.* (1969) and Elliott *et al.* (1967), who used wavelength scanning monochromators

viewing the nadir atmosphere. These were followed by a similar experiment on the OGO-4 satellite in 1967 (Anderson *et al.* 1969), in which data were collected over a 17-month period. The first major backscatter u.v. experiment with an instrument dedicated to ozone measurements was the b.u.v. on Nimbus 4 in a polar Sun-synchronous orbit. Launched in April 1970, this sensor continued to collect data until 1977. The instrument was a double monochromator which sampled 12 discrete wavelengths bands (Heath *et al.* 1973).

Residual Nimbus 4 b.u.v. hardware was later flown on the Atmospheric Explorer-5 spacecraft in November 1975, with an orbital inclination of 20°. Tropical data were collected and local time ozone changes were determined.

The most recent b.u.v. experiment is the Nimbus 7 s.b.u.v./t.o.m.s., launched in October 1978, in a Sun-synchronous polar orbit. This dual instrument continues the Nimbus 4 nadir ozone data set with the solar backscatter u.v. sensor (s.b.u.v.) (an improved version of the Nimbus 4 sensor) and adds spatial scanning of total ozone with the total ozone mapping spectrometer (t.o.m.s.).

Infrared emission methods for remote measurement of ozone are of two types (see table 1). Ozone profiles are determined from measurements of the altitude variation of the atmospheric radiance by viewing the Earth's limb (the limb radiance technique) and total ozone can be inferred from measurements of the atmospheric radiance in the nadir direction. The nadir sounding method was first tested on the Nimbus 3 satellite with an infrared interferometer spectrometer (i.r.i.s.) (Hanel *et al.* 1970). This was followed by a repeat flight on Nimbus 4. The retrieval methods and results were reported by Prabhakara *et al.* (1976).

The limb emission method is a more recent development, which has the advantages of good vertical resolution and simultaneous information about air temperature. Retrieval methods have been developed by Gille & House (1971) and the system has flown on the Nimbus 6 and 7 satellites.

Occultation techniques and results

Limb absorption or occultation measurements have been made with either the Sun or stars as the light source. Ozone profiles have been determined between about 40 and 100 km, thus giving the technique the distinction of working to higher altitudes than any other current sounding technique. Atmospheric attenutation is measured and subsequently interpreted in terms of Rayleigh scattering, atmospheric refraction and ozone slant path optical depth. Stellar occultations can, in principal, be obtained at any local time, although only night observations have been made with existing instrumentation. They are capable of high vertical resolution but are limited by the availability of suitable stars.

Solar occultation measurements are possible from a spacecraft sensor within an hour of sunrise or sunset at the ground twice during each orbit. The geographic coverage is rather severely limited by the orbit geometry. The vertical resolution is about 15 km unless the field of view is limited with a pointed telescope. The useful altitude range is determined by the number of wavelength channels, and the accuracy does not depend on absolute system calibration, but only on an electronic linearity and noise, and errors in effective ozone absorption coefficients.

The published results from occultation experiments are listed with references in table 1 and, since the quantity of soundings is small, the principal results are shown in figure 1 where the profiles are identified by the satellite name.

PHILOSOPHICAL TRANSACTIONS OF THE ROYAL SOCIETY A MATHEMATICAL, PHYSICAL & ENGINEERING SCIENCES

The K–M mid-latitude ozone model, (Krueger & Minzner 1976) which, for altitudes above 60 km, is derived primarily from twilight rocket flights, is also shown for comparison. The satellite profiles apply to a variety of latitudes, seasons and phases of the solar cycle and, as noted above, were obtained under near twilight or night conditions.

Night-time profiles from the orbiting astronomical observatories, OAO-2 and -3 show strong secondary maxima centered near 85 km and 95 km respectively. The OAO-3 results have been somewhat enigmatic because, at least below 80 km, the ozone densities are more than a factor of 2 greater than the results from the twilight experiments. If true, they would imply a night-time doubling in ozone density even at 50 km. The OAO-2 results exhibit the opposite effect below 75 km, namely a night-time ozone decrease relative to twilight measurements. The band of observed profiles from OAO-2 lies about a factor of 4 less than the K–M mid-latitude model at 50 km and appears to diverge at lower altitudes. The differences between the two OAO experiment results, and between them and the twilight results, are much greater than has been predicted for diurnal variations in the stratosphere and mesosphere.

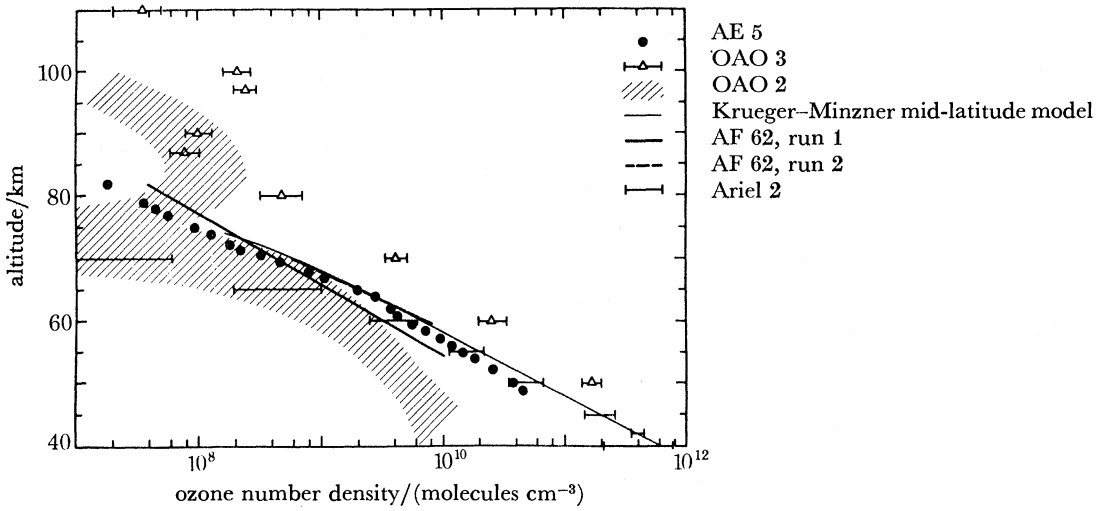

FIGURE 1. A comparison of ozone density distributions obtained with solar and stellar occultation methods.

The AE-5, AF 62, and Ariel 2 experiments are of the solar occultation type and, except for Ariel 2 at upper levels, the results tend to agree with the K–M mid-latitude model. The Ariel 2 data diverge toward lower values at higher altitudes and are consistent with the OAO-2 data at 65 and 70 km. The AE-5 results are 20–50 % less than the K-M mid-latitude model below 65 km. At those levels the K–M model becomes progressively more weighted toward daytime values. The AF 62 experiment determined only a two parameter profile, but two separate analysis techniques yielded different profiles (run 1 and run 2 in figure 1). The ozone densities from the AF 62 run 2 are quite close to AE-5 and K–M model results.

In summary, the solar occultation experiments differ significantly between themselves and from the rocket-derived K–M mid-latitude model. The ozone distribution shows a monotonic decrease with altitude with a scale height between 4 and 5 km for altitudes between 50 and 80 km. The ozone densities decrease from perhaps 5×10^{10} cm^{-3} at 50 km to about 1×10^8 cm^{-3} at 75 km. The differences from the K–M model at 50 km may be due to latitude gradients, since most of the occultation results come from near the equator.

The stellar occultation results, taken at night, would require an extraordinarily variable

mesosphere to account for the 10- to 100-fold differences in their profiles. These profiles are particularly hard to accept near 50 km, where a relative wealth of other data exists.

Clearly, the occultation techniques are still in a developmental stage and mesospheric ozone profiles and fields have not been adequately determined.

The backscatter ultraviolet (b.u.v.) method

The b.u.v. method has proved to be a useful technique for observing global characteristics of the high altitude ozone field. The technique is successful owing to the intense ozone absorption continuum in the middle ultraviolet, the apparent lack of contamination of this band by interfering species and the demonstrated lifetime of the satellite hardware. The principal shortcoming is the inability to resolve-structure in the ozone profile less than about an atmospheric scale height. This, incidentally, is not a severe drawback due to the general 'well behaved' nature of the ozone distribution in the upper stratosphere. However, no information is returned about the ozone distribution below the ozone maximum, although total ozone can be determined.

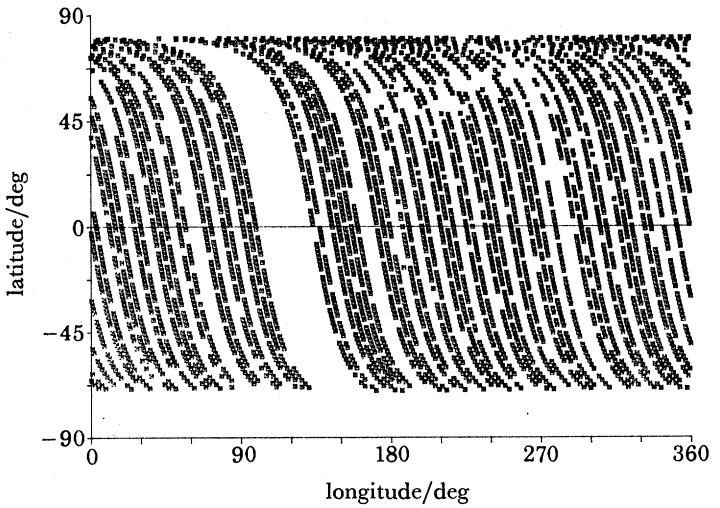

Figure 2. Data coverage for a typical week of b.u.v. data. Each square represents a b.u.v. sounding.

The inference of total ozone amounts and its vertical distribution is possible by solution of an integral equation. The fundamental observed parameters are the incident u.v. solar spectral irradiance and the atmospheric spectral radiance in the middle u.v. (250–340 nm). In addition, the surface reflectance must be determined by measurements at a wavelength that is free of ozone absorption. The wavelength dependence of the ozone absorption coefficient and the exponential decrease of air density with height leads to a series of contribution functions peaking at different levels corresponding to different wavelengths between 250 and 300 nm. The ozone profile can be inferred by using this altitude separation. At wavelengths greater than 300 nm, the contribution functions peak below the stratosphere and a total ozone measurement is possible.

Design of a spectrometer to measure the atmospheric radiance is difficult because the Earth's albedo changes drastically with wavelength between 250 and 340 nm, owing to ozone absorption. Furthermore, the solar flux is a factor of 10 less at 250 nm that it is at 340 nm. As a result, in a spectral scan of the earth radiance, the flux changes by 10^4. Further, observational

complications come from polarization of the backscattered light. To meet these stringent observational requirements, the Nimbus b.u.v. instruments are double (tandem) Ebert–Fastie monochrometers with collinear narrow-band filter photometers. The instrument views the terrestrial atmosphere at the nadir. At the northern terminator, a diffuser plate is deployed to compare the solar spectral irradiance to the atmospheric radiance.

The Nimbus 4 Backscatter Ultraviolet (b.u.v.) experiment was launched in April of 1970. The spacecraft is in a near polar Sun synchronous orbit and data are available over almost all of the sunlit portion of the earth with the observations taken near local noon. Coverage for a typical week is shown in figure 2 where each 200 km by 200 km sounding is represented by $\times$. There are an average of 800 data points per day for the first year of operations. Increasingly severe spacecraft power problems starting in July 1972 have caused a substantial reduction in operating time for the instrument although data are still occasionally collected from it.

Vertical profile results from b.u.v. observations

The first experiment in the development of the backscatter u.v. methods used a single channel photometer. Rawcliffe & Elliott (1966) inferred from the radiance data that seasonal differences were present in upper stratospheric ozone. The first findings from an ozone profile experiment using an ultraviolet spectrometer were that the upper stratospheric ozone scale height was constant at sub-polar latitudes and that detailed horizontal structure existed near 30 mbar† (Iozenas *et al.* 1969). These results indicated that photochemistry prevailed over dynamics at the upper levels. In succeeding experiments with spectrometers, it was suggested that instrument calibration uncertainties or possible aerosol scattering might present real problems for accurate estimation of ozone profiles (Elliott 1971). However, Anderson *et al.* (1969) found that profiles could be recovered after calibration with rocket ozone data and that latitudinal and seasonal ozone variations could nevertheless be determined (London *et al.* 1977). In the two data periods (Sept.–Nov. 1967 and Jan.–Feb. 1968) that have been analysed from the OGO-4 experiments, the average ozone fields at 5 mbar were found to have small geographic variations. A broad maximum appears at mid-latitudes and, in the tropics, some longitudinal asymmetry is present with higher ozone mixing ratios over the Atlantic and Africa. These geographical variations diminish with altitude in agreement with the earlier observations. The mixing ratios at higher latitudes were found to increase from autumn to winter.

Initial analysis of the Nimbus 4 ozone profile data (Krueger *et al.* 1973) revealed that the highest mixing ratios were near 10 mbar at lower latitudes. During the equinoxes, the mixing ratios decrease rather uniformly toward the poles. However, during the autumn and winter secondary maxima form near the 2 mbar level at Southern Hemisphere mid-latitudes and at Northern Hemisphere high latitudes. Perhaps the simplest explanation of these upper stratospheric features lies in the temperature dependence of the ozone chemistry. The southern maximum, in particular, was found to vary in amplitude at different longitudes. Barnett *et al.* (1975) used these b.u.v. results, together with s.c.r. temperature data, to estimate the temperature coefficient for steady state ozone mixing ratios. They concluded that the exponential coefficient was of the order of 900–1100 K, a value consistent with oxygen and hydroxyl chemistry near 1 mbar.

The Nimbus 4 b.u.v. was also taking data during the major solar proton event of August 1972. Ozone decreases of 20 % were found at 2 mbar in the upper stratosphere at geomagnetic

† 1 mbar = 10^2 Pa.

PHILOSOPHICAL TRANSACTIONS OF THE ROYAL SOCIETY A MATHEMATICAL, PHYSICAL & ENGINEERING SCIENCES

latitudes irradiated by protons (Heath *et al.* 1977). This was the first direct evidence for catalysis of ozone by odd nitrogen compounds in the stratosphere.

Methods for improvement of retrievals of high level ozone profiles from reprocessed b.u.v. Earth albedo data are currently under study. This new data set incorporates corrections for instrument sensitivity changes and spacecraft attitude errors. The aerosol effects found earlier by Elliott (1971) do not appear in Nimbus 4 b.u.v. data, although anomalous radiances appear to exist at 255 nm. Recently, the global behaviour of 1 mbar ozone from April 1970 to May 1972 has been studied at Goddard Space Flight Center by using an interim inversion product that is valid for the upper stratosphere – Mateer's formulation of the Laplace transform method (Twomey 1961). The variation of the zonal mean of the 1 mbar ozone mixing ratio at 60 N for the period Nov. 1970–Nov. 1971 is shown in figure 3. The 2 mbar air temperatures for the same latitude band and time period derived from s.c.r. observations (Barnett 1974) are shown in the same figure. Both b.u.v. and s.c.r. observe the radiation from rather broad height regions so the excellent inverse relationship of temperature and ozone is quite pleasing.

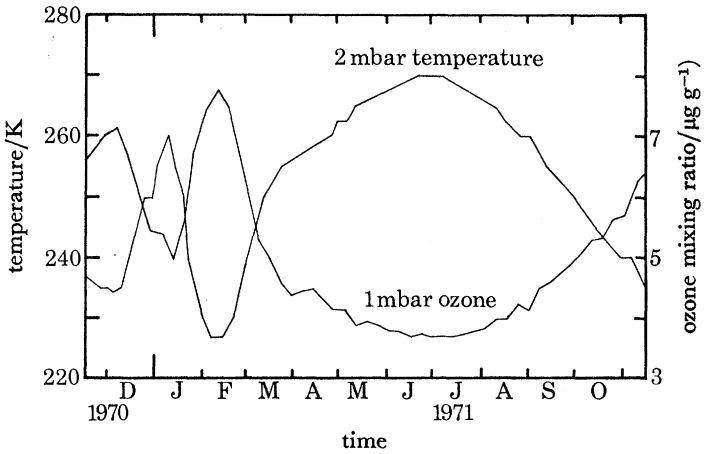

FIGURE 3. Temporal variation of the 2 mbar temperature from s.c.r. and the 1 mbar ozone mass mixing ratio in a latitude band centred at 60° N from 1 year of Nimbus 4 data.

The overall behaviour observed is a summer temperature maximum (270 K) and ozone minimum (3.71 μg/g) and a winter temperature minimum (227 K) and ozone maximum (7.62 μg/g). The large sudden stratospheric warming from mid-December to mid-January is mirrored exactly as a decrease in 1 mbar ozone. Even a small scale feature at the beginning of September is observed in both temperature and ozone. Temperature (T) and the ozone mixing ratio (r_3) are found to be related by the equation

$$r_3 = 0.072 \exp(1062/T)$$

with a correlation coefficient of 0.991 for the fit. This relation holds for the entire year except during the stratospheric warming, when the pre-exponential coefficient 0.072 μg/g increases to 0.082 μg/g. The temperature coefficient of 1062 K compares reasonably well with the value of 928 K reported by Barnett *et al.* (1975) at 50 S, but the correlation coefficient they report of 0.817 is substantially lower. This is due in part to our using much better calibrated ozone data and in part to using zonally averaged data. The increase in the pre-exponential coefficient during the stratospheric warming period is evidence for modification of the chemistry and dynamics from that normally present. This could happen if significant vertical motions arise.

Data from the AE-5 b.u.v. have been partially analysed. Principal findings to date are:

(1) the tropical profiles are consistent with current photochemical model results below 2 mbar but not higher altitudes (Frederick *et al.* 1978).

(2) the transition from dynamic to photochemical control of the ozone takes place between 5 and 10 mbar in the tropics (Frederick *et al.* 1977*b*) and

(3) negligible spatial structure exists in the integral ozone above 1 mbar at tropical latitudes when measured with 25 km horizontal resolution (Guenther & Dasgupta 1979).

TABLE 2. B.U.V./DOBSON OVERALL COMPARISON STATISTICS CHART

Year 1 (April 1970–April 1971)	number of coincidences	$\bar{\Omega}_N$ (m atm-cm)	$\bar{\Omega}_D$ (m atm-cm)	bias $(\bar{\Omega}_N - \bar{\Omega}_D)$	s.d.
Dobson 00 code, 2° sep, all R;	2024	315.9	326.4	−10.6	18.44
1° sep, $R \leqslant 0.2$	328	304.9	316.6	−11.8	16.28
all codes	3860	325.6	336.4	−10.9	21.29
all codes exc. 00 code	1841	336.4	347.7	−11.3	24.02
M-83 Network†	1270	349.7	358.8	−9.1	59.50
Year 2 (May 1971–April 1972)					
Dobson 00 code, 2° sep, all R;	1944	304.0	317.9	−13.9	18.83
1° sep, $R \leqslant 0.2$	301	292.0	304.4	−12.4	16.26
all codes	3392	313.9	329.2	−15.4	20.57
all codes exc. 00 code	1487	327.3	344.2	−17.0	23.65
M-83 network†	1117	342.3	368.9	−26.6	51.51

† Non-Dobson Russian filter photometer.

Total ozone from b.u.v. observations

The first application of the Dave & Mateer (1967) method for total ozone estimation from u.v. earth albedo measurements was on the Nimbus 4 b.u.v. Samples of the data were processed to establish the feasibility of the technique (Mateer *et al.* 1971) and to indicate the nature of time variations in the global ozone field (Krueger 1974). In 1976, as a result of the increasing importance of accurate monitoring of global ozone, a special effort was organized to process all the available data with the best possible accuracy. This effort included development of improved processing algorithms, compensation for instrument changes with ageing, careful review of the spacecraft ephemeris and attitude data and quality control of the output data. All the total ozone data have been reprocessed and archived in the National Space Sciences Data Center. Specific information as to how to acquire the processed Nimbus 4 total ozone data may be obtained by writing to World Data Center for Rockets and Satellites, Code 601, Goddard Space Flight Center, Greenbelt, Md. 20771, United States of America. There has been an extensive effort to assess the quality of the resulting data set. The primary comparison has been with the ozone measurements obtained from *Ozone data for the world* as provided by the Atmospheric Environment Services of Canada. All available spacecraft and ground data collocations have been identified and a variety of statistics computed. Results from several cases for the first 2 years are shown in table 2. All possible cases meeting the collocation criteria are included in each line with no preselection of either the ground or spacecraft data. The first line for each year is for AD-direct Sun wavelength pair (00 code) observations taken on the same day, with the centre of the spacecraft field-of-view within 2° of the ground station. A scatter plot of this set of data is shown in figure 4. The second line in the table 2 categories is a subset of the first,

with a colocation limit of 1° and only cases where the spacecraft scene is cloud free are included. The third line includes all types of Dobson data and the fourth line is a subset of the third in which all except the 00 code data are included. A similar comparison of b.u.v. data and M-83 data is shown in the last line for each year. There are four major types of errors that contribute to the overall variance between b.u.v. and ground data shown in this table: random errors in the b.u.v. data; random errors in the ground data; noise introduced by imperfect colocation in time, space and area sampled; and noise resulting from the apparent biases of individual ground stations as shown in the Dobson intercomparisons performed at Belsk and Boulder. It is not possible to establish how much of the bias between a specific ground station and the b.u.v. data originates in the ground station; however, is can be shown that roughly half the overall variance can be removed by nulling these biases out on a station by station basis. When reasonable estimates are made for each of the types of errors mentioned above, it appears that the b.u.v. data is similar in accuracy to a well run Dobson station.

Seasonal variations of total ozone have now been recomputed from the current b.u.v. data sets (Hilsenrath *et al.* 1978). A time–latitude cross section of zonally averaged total ozone was generated from average daily means for 10° wide latitude zones. In figure 5, the total ozone has been contoured with 20 m atm-cm increments for the 26-month period from April 1970

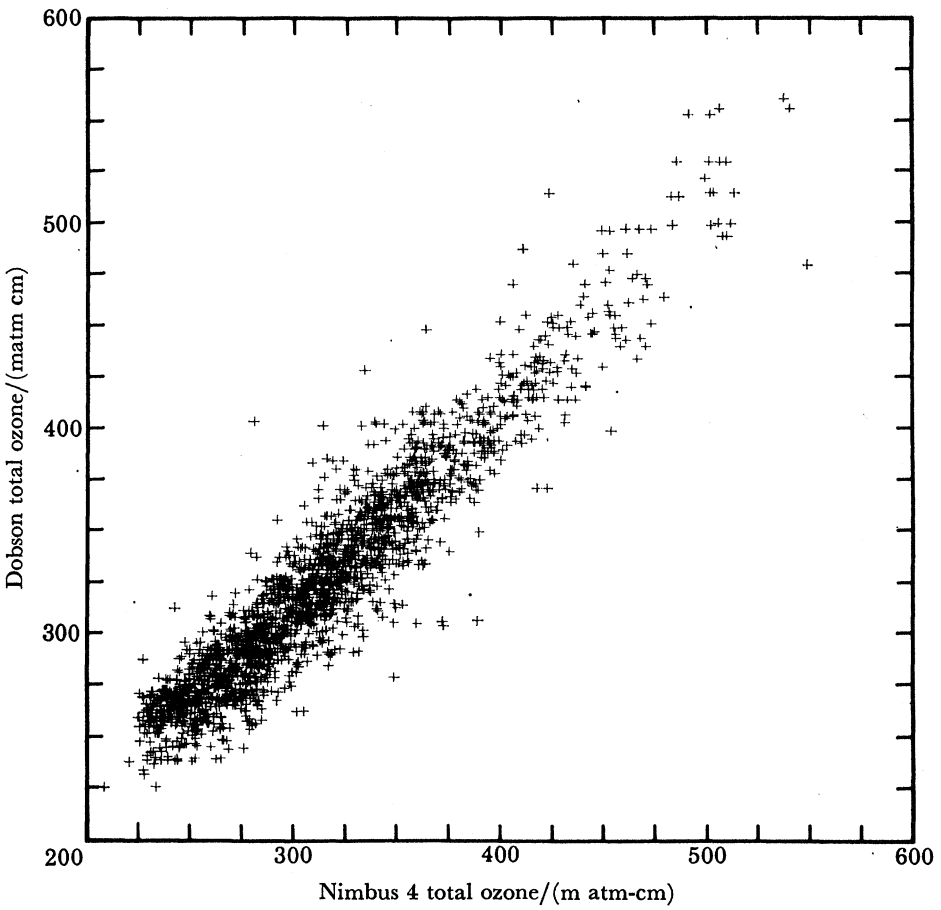

FIGURE 4. Comparison of b.u.v. total ozone estimations with coincident Dobson spectrophotometer total ozone measurements during the period 10 April 1970 to 30 April 1971. Only ADDS Dobson observations are included.

PHILOSOPHICAL TRANSACTIONS OF THE ROYAL SOCIETY A MATHEMATICAL, PHYSICAL & ENGINEERING SCIENCES

to May 1972 (contours are missing in the polar night because there are no observations during that period). The seasonal march of total ozone in the two hemispheres is clearly seen. A comparison with analyses of Dobson data (see, for example, London *et al.* 1976) reveals close correspondence with the major features in the ozone climatology. The b.u.v. results point up the distinctive differences in the seasonal trends for each hemisphere. These differences are as follows:

(1) In the Northern Hemisphere the spring maximum occurs nearly simultaneously at mid and high latitudes. The maximum value occurs near the pole, with total ozone amounts of about 500 m atm-cm in 1970 and decreasing to 460 and 440 m atm-cm in the spring of 1971 and 1972.

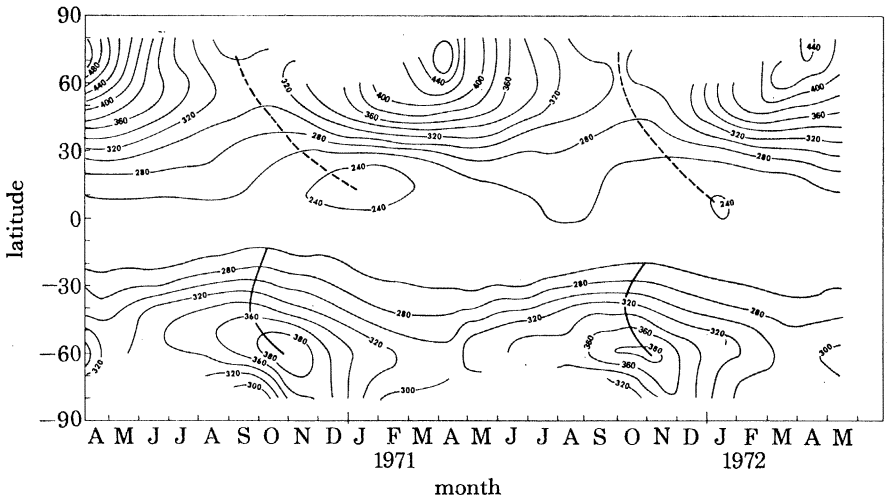

FIGURE 5. Time–latitude cross section of zonally averaged total ozone obtained from the Nimbus 4 b.u.v. from April 1970 to May 1972. The values are given in m atm-cm of ozone.

(2) In the Southern Hemisphere the spring build-up begins at 50 S in September with ozone values substantially lower than those in the Northern Hemisphere spring. The maximum values occur about 1 month later at polar latitudes. The asymmetry in the winter build-up in the two hemispheres is indicative of differences in the circulation features in the two hemispheres.

(3) In the tropical regions, the average total ozone amount is about 250 m atm-cm and a small seasonal variation is present, showing more rapid changes than in the long term Dobson averages. The ozone minimum, which is centred below the equator in April in both years moves northward after August. The lowest ozone amounts, which are found in the northern tropics, appear to follow after Southern Hemisphere spring maximum and are coincident with the Northern Hemisphere winter build-up.

A harmonic analysis has been made of the zonal mean data for the 2-year period (Hilsenrath *et al.* 1978). The results of this analysis are the following:

(1) More than 90 % of the variance of the zonal mean values at most latitudes is found in the two harmonics that represent the annual and semi-annual waves. The search for periodicities shorter than 1 month found no amplitudes greater than 5 m atm-cm at mid to high latitudes and 2 m atm-cm at low latitudes.

(2) At mid to high latitudes the annual wave dominates in both hemispheres. In the Northern Hemisphere the amplitude of the annual wave increases with latitude while in the Southern

Hemisphere the peak amplitude occurs at 50 S in the first year and at 60 S in the second year. The amplitude of the annual wave is a minimum at the equator in the first year and at 10 S in the second year. This shift in the minimum of the annual wave could be a result of the year to year change in the strength and location of the Hadley Cell circulation in the hemisphere.

(3) The semi-annual wave was observed at the higher latitudes in both hemispheres for the 2 years and in the tropics in the first year. This pattern is very similar to the analysis by London *et al.* (1976) of the Dobson data base. However, compared with the annual wave, the fractional variance in the semiannual wave is significant only in the tropics and at high southern latitudes. The tropical amplitude is small and probably is only an expression of the annual waves in the two hemispheres and, indeed, is in phase with these waves. The amplitude of the polar semi-annual wave is about 20 m atm-cm. This is comparable to the amplitude of the annual wave at 80 S but only a quarter of that amplitude at 80 N.

Infrared remote sensing of total ozone

The Nimbus 4 satellite carried an infrared interferometer spectrometer (i.r.i.s.), which provided measurements of the thermal emission spectrum of the Earth and atmosphere between about 400 and 1600 cm^{-1} with an apodized spectral resolution of 2.8 cm^{-1} (Hanel *et al.* 1971). The field of view of the instrument projected on the surface of the Earth was a circle with a diameter of approximately 95 km and all data were acquired near either local noon or local midnight between 80 N and 80 S. Measurements were essentially continuous from April to December 1970 and were available for a few days in January 1971.

The spectral measurements of i.r.i.s. in the 15 μm CO_2 band were inverted to derive the vertical distribution of temperature in the atmosphere (Conrath 1972). Using these temperature data, together with i.r.i.s. spectral measurements in the 9.6 μm ozone band, Prabhakara *et al.* (1976) deduced the global distribution of total ozone for about 10 months.

Though the i.r.i.s. was not a dedicated experiment for ozone soundings, the 9.6 μm band basically yields one parameter about ozone. This parameter depends both on the total ozone and its vertical distribution. Therefore, additional information must be provided to obtain total ozone explicitly. This additional information is provided by an empirical relation, based on balloon observations, which implies that increases in total ozone occur mainly because of increases in ozone concentration in the layers of the atmosphere below the ozone maximum. This empiricism and the crude vertical resolution, approximately 1 scale height, of the remotely sensed temperature profile in the lower stratosphere lead to a basic limitation on the infrared ozone remote sensing technique described by Prabhakara *et al.* (1976).

Since the time of the i.r.i.s flights, several temperature sounding instruments have included a channel to sense the 9.6 μm ozone band. Beginning in March 1977, the multichannel filter radiometer instruments on four of the Defense Meteorological Satellite Program series of satellites has included such a channel. Lovill *et al.* (1978) have reported preliminary results. The most recent 9.6 μm ozone sensor is part of the high resolution infrared radiometer (h.i.r.s.) sensor on the Tiros N Satellite, launched in November 1978.

Despite the limitations of the nadir infrared method, good coverage of the satellite data over the globe permit us to get some gross information on the geographic and seasonal variation of total ozone. The sensing capability at night and in the polar night could be very useful.

In figure 6, a map of the global distribution of ozone derived from i.r.i.s. for the month of December 1970 is shown to highlight the ozone information over the northern polar latitudes

PHILOSOPHICAL TRANSACTIONS OF THE ROYAL SOCIETY A MATHEMATICAL, PHYSICAL & ENGINEERING SCIENCES

in winter. Longitudinal changes of about 100 m atm-cm can be seen between the maximum values east of Siberia and the minimum values in the North Atlantic. In the tropics the lowest values appear in the Indonesian sector, perhaps in association with the Siberian ozone high. The tropical ozone tends to have a wavenumber 1 characteristic throughout the year with the maximum over the Atlantic as shown in the December chart. The maximum amplitude of this wave is in July and August.

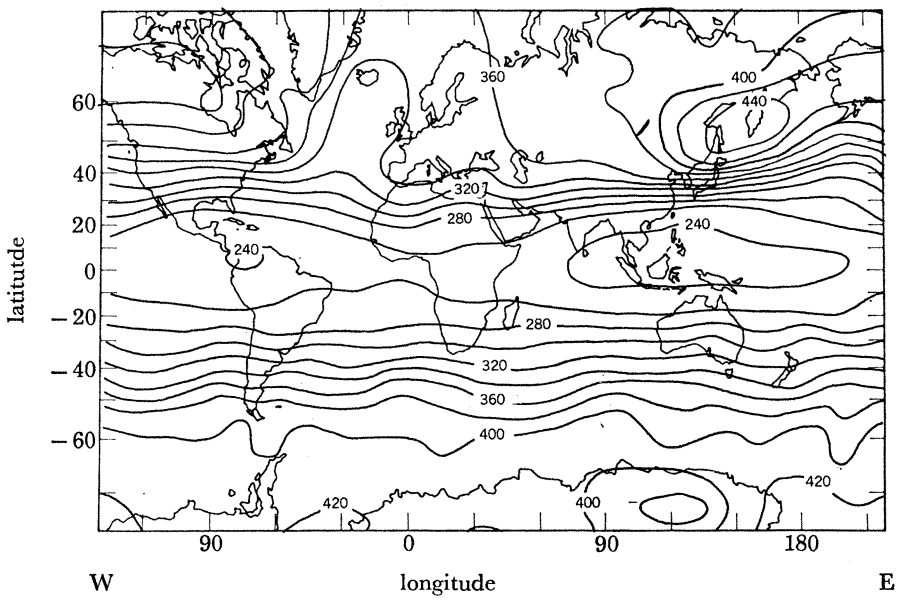

FIGURE 6. Mean global distribution of total ozone for December 1970 obtained from the Nimbus 4 i.r.i.s. instrument. The values are given in m atm-cm of ozone.

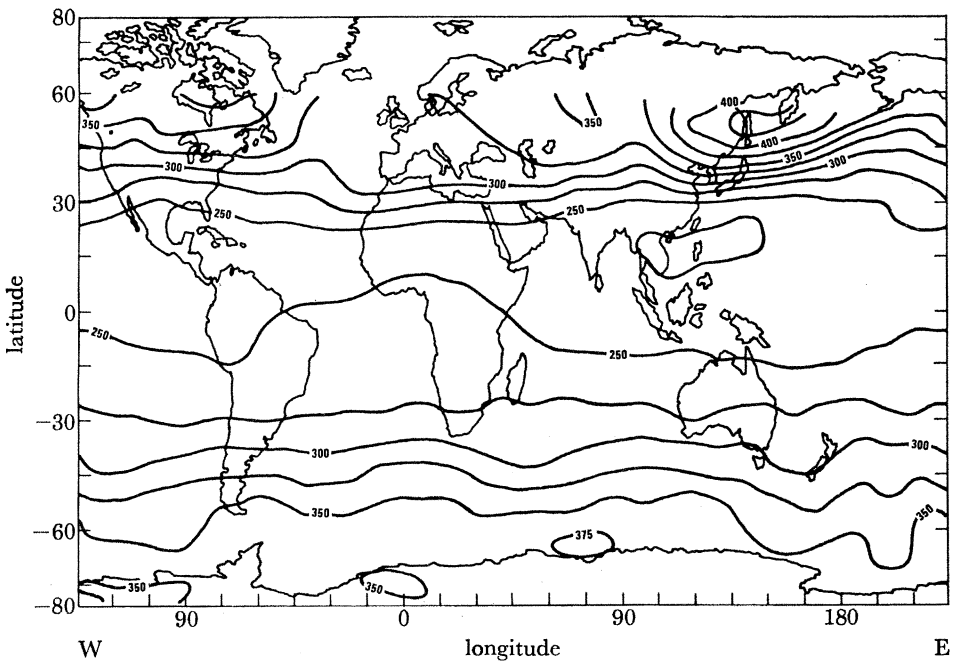

FIGURE 7. Mean global distribution of total ozone for December 1970 obtained from the Nimbus 4 b.u.v. instrument. The values are given in m atm-cm ozone. This chart may be compared with figure 6.

In the Southern Hemisphere, the December (summer) ozone field is fairly uniform at all latitudes except for the Antarctic regions. The i.r.i.s. December map exhibits a 40 m atm-cm zonal variation with the minimum located at the same longitude as the tropical minimum.

Comparative results from b.u.v. and i.r.i.s.

A comparison of the ozone results from i.r.i.s. and b.u.v. is of interest. Figure 7 is a December map of total ozone derived from the Nimbus 4 b.u.v. instrument. This can be compared directly with the map derived from i.r.i.s. (figure 6). In general the observed ozone features from the two instruments are the same. Taking into account the different contour intervals in the two maps, however, some differences in the absolute values can be found. This is expected from the study performed by Prabhakara *et al.* (1976), who demonstrate a reduction in the seasonal amplitude of the i.r.i.s. total ozone amounts. The two satellite measurements compare well in the tropics. The absolute amounts are very close and the minima occurring over Central America and Indonesia are observed by both instruments. In the Southern Hemisphere both measurements show a uniform latitude gradient from low to high latitudes; however, the b.u.v. values are about 15 % lower than the i.r.i.s. values. In the Northern Hemisphere the ozone high east of Siberia and the features in the North Atlantic are detected by both instruments. The absolute values agree here a little better than in the Southern Hemisphere.

Although the two instruments were on the same satellite, the data bases for these maps are not identical. B.u.v. observations are possible only in daytime, while i.r.i.s. soundings are taken day and night and, in addition, during the polar night. Furthermore, the instrument duty cycles were not identical and the data recovery varied between i.r.i.s. and b.u.v. However, it is encouraging that the features are reproduced since the measurement techniques are vastly different.

Conclusions

During the 1960s and into the 1970s, several methods for remote measurement of ozone were devised and tested. The most promising techniques for stratospheric soundings in the 1980s seem to be the backscatter u.v. system for ozone profile and total ozone monitoring and the limb infrared emission system for investigations requiring good vertical resolution of the ozone profile and complementary information on air temperatures and trace constituents. For mesospheric ozone measurements, the occultation methods have shown promise, although the unreasonable differences existing between experimental results must be resolved.

At present, several data sets have been collected and climatological descriptions are being assembled. The interpretation of these results in terms of atmospheric processes is only beginning. Already, photochemical modelling has been guided and theories tested by the satellite data. The ultimate utility will perhaps be found after the chemistry is well understood. At that point the global ozone data can be used for tracing air motions as a complementary source of information for dynamic models of the atmosphere.

PHILOSOPHICAL TRANSACTIONS OF THE ROYAL SOCIETY A MATHEMATICAL, PHYSICAL & ENGINEERING SCIENCES

References (Krueger *et al.*)

Anderson, G. P., Barth, C. A., Cayla, F. & London, J. 1969 *Ann. Geophys.* **25**, 239–243.

Barnett, J. J. 1974 *Qt. Jl R. met. Soc* **100**, 505–530.

Barnett, J. J., Houghton, J. T. & Pyle, J. A. 1975 *Jl R. met. Soc* **101**, 245–257.

Conrath, B. J. 1972 *J. atmos. Sci.* **29**, 1262–1271.

Dave, J. V. & Mateer, C. L. 1967 *J. atmos. Sci* **24**, 414–427.

Elliott, D. D., Clark, M. A. & Hudson, R. D. 1967 *Aerospace Techn. Report no.* TR-0158 (3260–10), 2 September 1967.

Elliott, D. D. 1971 *Space Research* XI, pp. 857–861. Berlin: Akademie–Verlag.

Frederick, J. E., Hays, P. B., Guenther, B. W. & Heath, D. F. 1977*a* *J. atmos. Sci.* **34**, 1987–1994.

Frederick, J. E., Guenther, B. W. & Heath, D. F. 1977*b* *Beitr. Phys. Atmos.* **50**, 496–507.

Frederick, J. E., Guenther, B., Hays, P. B. & Heath, D. F. 1978 *J. geophys. Res.* **83**, 953–958.

Gille, J. C. & House, F. B. 1971 *J. atmos. Sci.* **28**, 1427–1442.

Guenther, B. & Dasgupta, R. 1979 In preparation.

Guenther, B., Dasgupta, R. & Heath, D. F. 1977 *Geophys. Res. Lett.* **4**, 434–437.

Hanel, R. A., Schlachman, B., Clark, F. D., Prokesh, C. H., Taylor, J. B., Wilson, W. M. & Chaney, L. 1970 *Appl. Opt.* **9**, 1767–1774.

Hanel, R. A., Shlachman, B., Rogers, D. & Vanouse, D. 1971 *Appl. Opt.* **10**, 1376–1382.

Hays, P. B. & Roble, R. G. 1973 *Planet. Space Sci.* **21**, 273–279.

Heath, D. F., Mateer, C. L. & Krueger, A. J. 1973 *Pure appl. Geophys.* **106–108**, 1239–1253.

Heath, D. F., Krueger, A. J., Roeder, H. A. & Henderson, B. D. 1975 *Opt. Engng* **14**, 323–331.

Heath, D. F., Krueger, A. J. & Crutzen, P. J. 1977 *Science N.Y.* **197**, 323–331.

Hilsenrath, E., Heath, D. F. & Schlesinger, B. M. 1979 *J. geophys. Res.* **84**. (In the press.)

Iozenas, V. A., Krasnopol'skiy, V. A., Kuznetsov, A. P. & Lebedinsky, A. I. 1969 *Atmos. oceanic Phys.* **5**, 149–159.

Krueger, A. J. 1974 *Proc. Int. Conf. on Structure, Composition and General Circulation of the Upper and Lower Atmosphere and Possible Anthropogenic Perturbations*, vol. 1, pp. 467–477.

Krueger, A. J., Heath, D. F. & Mateer, C. L. 1973 *Pure appl. Geophys.* **106–108**, 1254–1263.

Krueger, A. J. & Minzer, R. A. 1976 *J. geophys. Res.* **81**, 4477–4481.

London, J., Bojkov, R. D., Oltmans, S. & Kelley, J. I. 1976 *N.C.A.R. Tech. Note* TN/113+STR. National Center for Atmospheric Research, Boulder, Colorado.

London, J., Frederick, J. E. & Anderson, G. P. 1977 *J. geophys. Res.* **82**, 2543–2556.

Lovill, J. E., Sullivan, T. J., Weichel, R. L., Ellis, J. S., Huebel, J. G., Korver, J. A., Werdhaas, P. P. & Phelps, F. A. 1978 *Lawrence Livermore Laboratory* UCRL-52473, May 25.

Mateer, C. L. 1972 In *Mathematics of profile inversion* (ed. L. Colin), pp. 2–25. N.A.S.A.TMX-62,150.

Mateer, C. L., Heath, D. F. & Krueger, A. J. 1971 *J. atmos. Sci.* **28**, 1307–1311.

Miller, D. E. & Steward, K. H. 1965 *Proc. R. Soc. Lond.* A**288**, 540–544.

Nimbus Project 1978 *The Nimbus 7 Users Guide*, NASA, Goddard Space Flight Center, Greenbelt, Md.

Prabhakara, C., Rodgers, E. B., Conrath, B. J., Hanel, R. A. & Kunde, V. G. 1976 *J. geophys. Res.* **81**, 6391–6399.

Rawcliffe, R. D., Meloy, G. E., Friedman, R. M. & Rogers, E. H. 1963 *J. geophys. Res.* **68**, 6425–6429.

Rawcliffe, R. D. & Elliott, D. D. 1966 *J. geophys. Res.* **71**, 5077–5089.

Riegler, G. R., Drake, J. F., Liu, S. C. & Cicerone, R. J. 1976 *J. geophys. Res.* **81**, 4997–5001.

Singer, S. F. & Wentworth, R. C. 1957 *J. geophys. Res.* **62**, 229–308.

Twomey, S. 1961 *J. geophys. Res.* **66**, 2153–2162.

Venkateswaran, S. V., Moore, J. G. & Krueger, A. J. 1961 *J. geophys. Res.* **66**, 1751–1771.

PHILOSOPHICAL TRANSACTIONS OF THE ROYAL SOCIETY A MATHEMATICAL, PHYSICAL & ENGINEERING SCIENCES